

Machine Modelling for Transient Stability Analysis in Distribution Grids

A Comparison of Synchronous and Induction Machine Models in Medium and Low Voltage Grids

Johannes Weidner and Lutz Hofmann

Institute of Electric Power Systems, Leibniz University Hannover, Appelstraße 9a, Hannover, Germany

Keywords: Transient Stability, Distribution Grid, Machine Modelling, Distributed Generation.

Abstract: The complete models for synchronous and induction machines are compared with selected approximated models. This is to validate the approximations for the utilisation in transient stability analysis in distribution grids. The results show that they can be used to simulate stable oscillations, but they lose their accuracy approaching the area of transient instability. The main reason is the active power exchange during faults, which is not jumping to zero as it does in high voltage scenarios.

1 INTRODUCTION

The installed power of distributed generation units in the medium and low voltage grids is continuously increasing. Substituting conventional technologies, reliability and stability of these units has to increase proportional. Therefore the consequences to the stability in the resulting weakly meshed multi machine systems have to be analysed. This is not a standard procedure, since resistances of the grid cannot be neglected as in the high voltage grid. Additionally the machine parameters can have different relations to each other.

This paper is focused on the modelling of rotating machines in distribution grids under the perspective of transient stability analysis. This is done by comparing complete models for synchronous and induction machine with selected approximated models. The approximated models are equivalent to the standard transient model of synchronous machines (Kundur, 2007). These models are easy to use in initialisation and simulation, because they can be reduced to a mechanical equation system and an equivalent circuit with constant voltage source.

The aim is to validate these alternative models also for the utilization in transient stability analysis regarding distribution grids.

2 SIMULATION MODEL

The analysis is based on a simulation model, which is suitable for meshed grids. The equation system is taken from the literature and then modified to receive an approximated model with comparable parameters and variables. In this paper a simple test grid with one machine and its connection to the overlaying grid will be used to obtain a qualitative comparison of the investigated machine models. The scenario for the transient stability analysis assumes a 3-phase fault in the overlaying grid N, which the generator G should run through without transient instability.

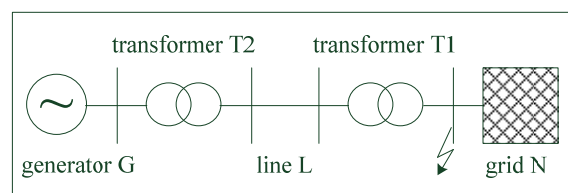


Figure 1: Topology of the basic scenario.

The complete model of the synchronous machine is taken from the literature. Other models were derived from the corresponding equation system to receive a formulation with similar parameters and variables. The natural behavior of the machine models is analyzed, so the excitation and the

mechanical torque were held constant during the simulations.

As component parameters typical values for voltage level and rated power were chosen. The rated parameters for the scenarios are listed below.

Table 1: Rated parameters for the scenarios.

	Parameter	Medium Voltage	Low Voltage
N	U_{nN}	110 kV	20 kV
	$S'_{k,N}$	6 GVA	0,5 GVA
T1	S_{rT1}	40 MVA	630 kVA
L	l_L	3 km	300 m
	type _L	AL/ST 3x50/8/20	NAYY 4x120/0
T2	S_{rT2}	2 MVA	-
G	U_{rG}	600 V	400 V
	S_{rG}	2 MVA	100 kVA

2.1 Electrical Grid

Due to the relatively small voltage in distribution grids the line capacities have only a small effect on the load flow and can be neglected for transient stability analysis.

The model is following the extended nodal method (Oswald, 2009) for resistive and inductive grids. Voltages and currents are formulated as space phasors \underline{g} which can be transformed from and to the momentary values of each phase g_a , g_b and g_c , using the complex phasor $\underline{a}=0,5(-1+j\sqrt{3})$.

$$\underline{g} = \begin{bmatrix} g_r \\ g_s \\ g_h \end{bmatrix} = \frac{2}{3} \begin{bmatrix} 1 & \underline{a} & \underline{a}^2 \\ 1 & \underline{a}^2 & \underline{a} \\ 1 & 1 & 1 \end{bmatrix} \begin{bmatrix} g_a \\ g_b \\ g_c \end{bmatrix} \quad (1)$$

All grid components, like transformers, lines and machines, consist of a reactance R_L , an inductance L_L and a voltage source \underline{u}_{qL} connected in series. Please note that considering the phase shifting of transformers L_L can be complex.

$$\underline{u}_L = R_L \underline{i}_L + L_L \dot{\underline{i}}_L + \underline{u}_{qL} \quad (2)$$

The connection between components and nodes is described by a coupling matrix K_{LL} . An algebraic equation is used to calculate the nodal voltages $\underline{u}_{L,all}$ from the currents $\underline{i}_{L,all}$ and voltage sources $\underline{u}_{qL,all}$ as vectors of all the components phasors.

$$\underline{u}_{L,all} = -K_{LL}^T (K_{LL} L_{L,all}^{-1} K_{LL}^T)^{-1} K_{LL} L_{L,all}^{-1} \cdot (R_{L,all} \underline{i}_{L,all} + \underline{u}_{qL,all}) \quad (3)$$

The voltage sources are either defined by the input data or calculated from the state variables of the components.

2.1.1 Complete Model

In the complete model the currents of inductances are state variables. From the voltage equation of each component, the differential equation for the currents can easily be obtained.

$$\dot{\underline{i}}_L = L_L^{-1} (\underline{u}_L - R_L \underline{i}_L - \underline{u}_{qL}) \quad (4)$$

2.1.2 Approximated Model

The state variables of the grid can be assumed as steady state. In this case voltages and currents are sinusoidal with a constant grid frequency ω_N . In the formulation with rotating space phasors the derivative is imaginable as the tangent at the point of operation. For balanced conditions the space phasor is moving in a circle.

$$\dot{\underline{i}}_L = j\omega_N \underline{i}_L = \begin{bmatrix} j & 0 & 0 \\ 0 & -j & 0 \\ 0 & 0 & 0 \end{bmatrix} \omega_N \underline{i}_L \quad (5)$$

This leads to the formulation with complex impedances for the resistive and inductive branch.

$$\underline{u}_L = (R_L + j\omega_N L_L) \underline{i}_L + \underline{u}_{qL} \quad (6)$$

Because the nodal voltages $\underline{u}_{L,all}$ can be calculated from currents $\underline{i}_{L,all}$ and voltage sources $\underline{u}_{qL,all}$, the equations can be transposed to the steady state currents. Doing so a current depending part ΔZ of the voltage source has to be taken into account.

$$\underline{u}_{qL} = \Delta Z \underline{i}_L + \underline{u}'_{qL} \quad (7)$$

$$\underline{i}_{L,all} = - \left(j\omega_N L_{L,all} + M (R_{L,all} + \Delta Z_{all}) \right)^{-1} \cdot M \underline{u}'_{qL,all} \quad (8)$$

$$M = K_{LL}^T (K_{LL} L_{L,all}^{-1} K_{LL}^T)^{-1} K_{LL} L_{L,all}^{-1} + E \quad (9)$$

2.1.3 Simulation Parameters

The parameters are chosen to represent typical grid scenarios for a medium and a low voltage feed in, neglecting the parallel strings in a radial grid.

Table 2: Simulation parameters for the grid components referred to the nominal voltage of the considered grid.

Parameter	Medium Voltage	Low Voltage
R_N	0 Ω	0 Ω
L_N	0,23 mH	1,1 μ H
R_{T1}	25 m Ω	13,5 m Ω
L_{T1}	3,5 mH	2,8 mH
R_L	1,7 Ω	0,25 Ω
L_L	3,5 mH	0,31 mH
R_{T2}	1,5 Ω	-
L_{T2}	41 mH	-

2.2 Synchronous Machine (SM)

Synchronous machines are used in conventional power plants. Therefore a lot of models and analysis on their transient behaviour in high voltage grids exist. In distribution grids they are used to connect plants which operate with constant shaft frequency.

The model of the synchronous machine is made up of a resistance R_L , an inductance L_L and a controlled voltage source \underline{u}_{qL} connected in series.

2.2.1 Complete Model (SMc)

The equation system of the resistance the inductance, the controlled voltage source and the inner states of the machine is taken from (Hofmann, 2003). The considered eight state variables are:

- the three stator currents \underline{i}_L , modelled as rotating space phasors,
- the rotor flux linkages of the excitation winding Ψ_F as well as of the damping winding in the d-axis Ψ_D and in the q-axis Ψ_Q ,
- the angular frequency ω_{LF} and
- the angle of the rotor ϑ_{LF} .

The equations related to the coupling with the grid are written below. A magnetic saliency ($L_d'' \neq L_q''$) causes angle depending elements in the resistance and the inductance matrices.

$$\mathbf{R}_L = \begin{bmatrix} R_a & j\omega_{LF} \frac{L_d'' - L_q''}{e^{-2j\vartheta_{LF}}} & 0 \\ -j\omega_{LF} \frac{L_d'' - L_q''}{e^{2j\vartheta_{LF}}} & R_a & 0 \\ 0 & 0 & R_0 \end{bmatrix} \quad (10)$$

$$\mathbf{L}_L = \frac{1}{2} \begin{bmatrix} L_d'' + L_q'' & \frac{L_d'' - L_q''}{e^{-2j\vartheta_{LF}}} & 0 \\ \frac{L_d'' - L_q''}{e^{2j\vartheta_{LF}}} & L_d'' + L_q'' & 0 \\ 0 & 0 & 2L_0 \end{bmatrix} \quad (11)$$

$$\underline{u}_{qL} \approx \begin{bmatrix} e^{j\vartheta_{LF}} & 0 & 0 \\ 0 & e^{-j\vartheta_{LF}} & 0 \\ 0 & 0 & 1 \end{bmatrix} \left(\omega_{LF} \begin{bmatrix} j & j & -1 \\ -j & -j & -1 \\ 0 & 0 & 0 \end{bmatrix} - \begin{bmatrix} H_{FF} + H_{DF} & H_{DD} + H_{FD} & jH_{QQ} \\ H_{FF} + H_{DF} & H_{DD} + H_{FD} & -jH_{QQ} \\ 0 & 0 & 0 \end{bmatrix} \right) \begin{bmatrix} k_F \Psi_F \\ k_D \Psi_D \\ k_Q \Psi_Q \end{bmatrix} \quad (12)$$

The additional small effects of stator currents and excitation voltage on the voltage source are not shown in the equation.

The behaviour of the inner state variables is characterised by a differential equation system, using the Park-transformation for the stator currents.

$$\begin{bmatrix} \dot{i}_d \\ \dot{i}_q \\ \dot{i}_0 \end{bmatrix} = \frac{1}{2} \begin{bmatrix} 1 & 1 & 0 \\ -j & j & 0 \\ 1 & 0 & 2 \end{bmatrix} \begin{bmatrix} e^{-j\vartheta_{LF}} & 0 & 0 \\ 0 & e^{j\vartheta_{LF}} & 0 \\ 0 & 0 & 1 \end{bmatrix} \underline{i}_L \quad (13)$$

$$\begin{bmatrix} k_F \Psi_F \\ k_D \Psi_D \\ k_Q \Psi_Q \end{bmatrix} = - \begin{bmatrix} H_{FF} & H_{FD} & 0 \\ H_{DF} & H_{DD} & 0 \\ 0 & 0 & H_{QQ} \end{bmatrix} \begin{bmatrix} k_F \Psi_F \\ k_D \Psi_D \\ k_Q \Psi_Q \end{bmatrix} + \begin{bmatrix} k_F^2 R_F & 0 & 0 \\ k_D^2 R_D & 0 & 0 \\ 0 & k_Q^2 R_Q & 0 \end{bmatrix} \begin{bmatrix} i_d \\ i_q \\ i_0 \end{bmatrix} + \begin{bmatrix} k_F u_F \\ 0 \\ 0 \end{bmatrix} \quad (14)$$

$$m_e = \frac{3p}{2} \left((L_d'' - L_q'') i_d i_q + (k_F \Psi_F + k_D \Psi_D) i_q - k_Q \Psi_Q i_d \right) \quad (15)$$

$$\begin{bmatrix} \dot{\omega}_{LF} \\ \dot{\vartheta}_{LF} \end{bmatrix} = \begin{bmatrix} 0 & 0 \\ 1 & 0 \end{bmatrix} \begin{bmatrix} \omega_{LF} \\ \vartheta_{LF} \end{bmatrix} + \frac{p}{j} \begin{bmatrix} m_m + m_e \\ 0 \end{bmatrix} \quad (16)$$

The behavior of the machine is influenced by the turbine torque on the rotor shaft m_m and the excitation voltage u_F , which are both considered constant in this model.

2.2.2 Approximated Model (SMa)

In the conventional model for transient analysis the stator currents and the d-axis currents in the damping winding are considered to be steady state. This leads to a separation of the voltage source \underline{u}_{qL} in a inductive part $\Delta \mathbf{L}'$ and a transient voltage \underline{u}'_{qL} , which is considered to have a constant amplitude.

$$\underline{u}_L = \underline{u}'_{qL} + (\mathbf{R}_L + j\omega_{LF} \mathbf{L}_L + j\omega_{LF} \Delta \mathbf{L}') \underline{i}_L \quad (17)$$

Similar results can be obtained when the q-axis currents in the damping winding are also considered to be steady state. This leads to the advantage that the magnetic saliency can still be taken into account.

$$\Delta \mathbf{L}' = \frac{1}{2} \begin{bmatrix} \Delta L'_d + \Delta L'_q & \frac{\Delta L'_d - \Delta L'_q}{e^{-2j\vartheta_{LF}}} & 0 \\ \frac{\Delta L'_d - \Delta L'_q}{e^{2j\vartheta_{LF}}} & \Delta L'_d + \Delta L'_q & 0 \\ 0 & 0 & 0 \end{bmatrix} \quad (18)$$

$$\Delta L'_d = \frac{k_D^2 R_D}{H_{DD}} \quad (19)$$

$$\Delta L'_q = \frac{k_Q^2 R_Q}{H_{QQ}} \quad (20)$$

The transient voltage is constant when the rotor frequency and the flux linkages of the excitation winding do not change.

$$\begin{aligned} \underline{u}'_{qL} \approx & \left(\begin{matrix} H_{DD} & H_{FF} & -H_{DF} & H_{FD} \\ -j\omega_{LF} & (H_{DD} - H_{DF}) & & \\ & & & \end{matrix} \right) \begin{bmatrix} 1 \\ 1 \\ 0 \end{bmatrix} \\ & - \left(\begin{matrix} 1 \\ -1 \\ 0 \end{matrix} \right) \frac{k_F \Psi_F^0}{H_{DD}} \end{aligned} \quad (21)$$

The differential equation of the rotor flux linkages is substituted by an algebraic equation, depending on the stator currents and its initial value Ψ_F^0 .

$$\begin{bmatrix} k_F \Psi_F \\ k_D \Psi_D \\ k_Q \Psi_Q \end{bmatrix} = \begin{bmatrix} 1 \\ -H_{DF} \\ H_{DD} \\ 0 \end{bmatrix} k_F \Psi_F^0 + \begin{bmatrix} 0 & 0 \\ \Delta L'_d & 0 \\ 0 & \Delta L'_q \end{bmatrix} \begin{bmatrix} i_d \\ i_q \end{bmatrix} \quad (22)$$

Due to this constant flux linkage the number of state variables could be reduced to two variables.

The differential equations of rotor frequency and rotor angle are not directly changed, but the equation of the flux linkages can be inserted.

$$\begin{aligned} m_e = & \frac{3p}{2} \cdot \left((L'_d + \Delta L'_d - L'_q - \Delta L'_q) \cdot i_d i_q \right. \\ & \left. + \left(1 - \frac{H_{DF}}{H_{DD}} \right) \cdot k_F \Psi_F^0 \cdot i_q \right) \end{aligned} \quad (23)$$

2.2.3 Simulation Parameters

The parameters are chosen to represent typical values for synchronous machines with the designated rated power and voltage.

Table 3: Parameters for the synchronous generator referred to the nominal voltage of the considered grid.

Parameter	Medium Voltage	Low Voltage
R_a	2,2 Ω	57 m Ω
L_d''	73 mH	0,55 mH
L_q''	0,11 H	0,96 mH
H_{FF}	2,9 s ⁻¹	22 s ⁻¹
H_{DF}	-41 s ⁻¹	-61 s ⁻¹
H_{FD}	-2,7 s ⁻¹	-22 s ⁻¹
H_{DD}	43 s ⁻¹	64 s ⁻¹
H_{QQ}	8,3 s ⁻¹	20 s ⁻¹
R_F	0,53 Ω	22 m Ω
R_D	8,1 Ω	64 m Ω
R_Q	9,0 Ω	0,15 Ω
k_F	0,60	0,38
k_D	0,37	0,60
k_Q	0,86	0,82
p	2	2
J	57 kgm ²	1,1 kgm ²

2.3 Induction Machine (IM)

Besides inverters, where the transient behaviour can be chosen within the current and voltage limits, most of the generation units in distribution grids are connected to the grid via induction machines.

The models used in this paper are derived from the presented complete model of the synchronous machine. Therefore the excitation winding was extracted, the magnetic saliency was neglected and an excitation voltage for the remaining rotor winding was implemented (u_D and u_Q). In steady state operations this voltages are impressed with the slip frequency of the rotor.

2.3.1 Complete Model (IMc)

The model considers seven state variables:

- the three stator currents \underline{i}_L , modelled as rotating space,
- the rotor flux linkages of the rotor winding in the d-axis Ψ_D and in the q-axis Ψ_Q ,
- the angular frequency ω_{LF} and
- the angle of the rotor ϑ_{LF} .

Please note that the state variables can be reduced by the angle rotor, when there is no excitation voltage, or an excitation voltage which is always in phase with the rotor flux linkages.

The equations related to the coupling with the grid are relatively simple. This is caused by the symmetrical windings.

$$\mathbf{R}_L = \begin{bmatrix} R_a & 0 & 0 \\ 0 & R_a & 0 \\ 0 & 0 & R_0 \end{bmatrix} \quad (24)$$

$$\mathbf{L}_L = \begin{bmatrix} L'' & 0 & 0 \\ 0 & L'' & 0 \\ 0 & 0 & L_0 \end{bmatrix} \quad (25)$$

$$\mathbf{u}_{qL} = \begin{bmatrix} k_{LF}^2 R_{LF} & 0 & 0 \\ 0 & k_{LF}^2 R_{LF} & 0 \\ 0 & 0 & 0 \end{bmatrix} \mathbf{i}_L + \mathbf{T}_{PRa} \begin{bmatrix} k_{LF} u_d \\ k_{LF} u_q \end{bmatrix} + \frac{k_{LF}}{T_{LF}} \begin{bmatrix} 1+j\omega_{LF} T_{LF} & 0 & 0 \\ 0 & 1-j\omega_{LF} T_{LF} & 0 \\ 0 & 0 & 0 \end{bmatrix} \mathbf{T}_{PRa} \begin{bmatrix} \Psi_D \\ \Psi_Q \end{bmatrix} \quad (26)$$

The transformation matrix \mathbf{T}_{PRa} converts to the space phasor representation.

$$\mathbf{T}_{PRa} = \begin{bmatrix} e^{j\theta_{LF}} & 0 \\ 0 & e^{-j\theta_{LF}} \\ 0 & 0 \end{bmatrix} \begin{bmatrix} 1 & j \\ 1 & -j \end{bmatrix} \quad (27)$$

The behaviour of the inner state variables is characterised by a differential equation system, using the Park-transformation for the stator currents.

$$\begin{bmatrix} \dot{i}_d \\ \dot{i}_q \\ \dot{i}_0 \end{bmatrix} = \frac{1}{2} \begin{bmatrix} 1 & 1 & 0 \\ -j & j & 0 \\ 0 & 0 & 2 \end{bmatrix} \begin{bmatrix} e^{-j\theta_{LF}} & 0 & 0 \\ 0 & e^{j\theta_{LF}} & 0 \\ 0 & 0 & 1 \end{bmatrix} \mathbf{i}_L \quad (28)$$

$$\begin{bmatrix} k_{LF} \dot{\Psi}_D \\ k_{LF} \dot{\Psi}_Q \end{bmatrix} = \begin{bmatrix} k_{LF}^2 R_{LF} & 0 & 0 \\ 0 & k_{LF}^2 R_{LF} & 0 \end{bmatrix} \begin{bmatrix} i_d \\ i_q \\ i_0 \end{bmatrix} - \begin{bmatrix} 1 \\ T_{LF} & 0 \\ 0 & 1 \\ T_{LF} \end{bmatrix} \begin{bmatrix} k_{LF} \Psi_D \\ k_{LF} \Psi_Q \end{bmatrix} + \begin{bmatrix} k_{LF} u_D \\ k_{LF} u_Q \end{bmatrix} \quad (29)$$

$$m_e = \frac{3p}{2} (k_{LF} \Psi_D \cdot i_q - k_{LF} \Psi_Q \cdot i_d) \quad (30)$$

The equation of motion is similar to the synchronous machine. Though, the behavior of the machine is influenced by the mechanical torque on the rotor shaft m_m , which is considered to be constant in this model, and the excitation voltages in the rotor winding u_D and u_Q , which are assumed to rotate with slip frequency.

2.3.2 Approximated Model (IMa)

There is no classic model for the transient analysis of induction machines. Both, the steady state and the

short circuit model are not suitable in any scenario. Therefore an equivalent approach as for the synchronous machine is implemented. In the first step the stator currents are considered to be steady state and in the second step the amplitude of the rotor flux linkage Ψ is hold constant. This leads to a model with three state variables ω_{LF} , θ_{LF} and θ_Ψ , where θ_Ψ is the angle of the flux. The angles can be again combined to one variable, when there is no excitation voltage or when the excitation voltage is perfectly in phase with the flux linkage.

$$\psi^0 = |\Psi_D^0 + j\Psi_Q^0| \quad (31)$$

$$\theta_\Psi^0 = \angle(\Psi_D^0 + j\Psi_Q^0) \quad (32)$$

In the equivalent circuit on the grid side only the formulation of the flux linkage in the voltage source equation is changed.

$$\begin{bmatrix} k_{LF} \Psi_D \\ k_{LF} \Psi_Q \end{bmatrix} = k_{LF} \psi^0 \cdot \begin{bmatrix} \cos(\theta_\Psi) \\ \sin(\theta_\Psi) \end{bmatrix} \quad (33)$$

The differential equations of the inner state variables are formulated using the equation system of the complete machine model.

$$\dot{\theta}_\Psi = \frac{\dot{\Psi}_Q}{\psi^0} \cos(\theta_\Psi) - \frac{\dot{\Psi}_D}{\psi^0} \sin(\theta_\Psi) \quad (34)$$

$$m_e = \frac{3p}{2} (k_{LF} \psi^0 \cos(\theta_\Psi) i_q - k_{LF} \psi^0 \sin(\theta_\Psi) i_d) \quad (35)$$

2.3.3 Simulation Parameters

The parameters are chosen to represent typical values of induction machines with the designated rated power and voltage.

Table 4: Simulation parameters of the induction machine referred to the nominal voltage of the considered grid.

Parameter	Medium Voltage	Low Voltage
R_a	1,0 Ω	0,18 Ω
L''	0,13 H	0,76 mH
T_{LF}	2,0 s	0,56 s
R_{LF}	1,0 Ω	0,18 Ω
k_{LF}	0,97	0,96
p	2	3
J	108 kgm ²	1,2 kgm ²

3 SHORT CIRCUIT SIMULATION

Both machines and their approximated models where confronted with a short circuit in the

overlying grid. The aim is to compare the models on the basis of their transient behaviors. As explained below, the maximal amplitude of the voltage source angles (referred to the grid angle) during the oscillations are used as criterion to estimate the degree of transient stability. Please note, that it is only not an indicator for instability. Similar to the classic approach, always the coherence between the voltage angles has to be checked.

Based on the basic scenario, variations are included to gain a more abstract view on the model behaviors. The variations include:

- the duration of the fault,
- the residual voltage of the fault,
- the short circuit power,
- the rated power of the machine and
- the operation point of the machine.

The dependence on the rated power of the transformer is small and not shown separately.

3.1 Medium Voltage Scenario

The machine, connected to the medium voltage grid, has to withstand a short circuit at the 110-kV-side of the transformer T1, with a duration of 100 milliseconds.

3.1.1 Basic Scenario

The classic approach to analyze the transient stability is to analyze the developing of the rotor angles in relation to the grids angle center.

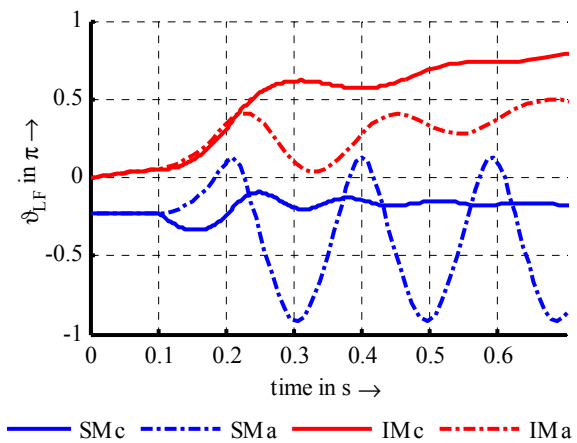


Figure 2: Rotor angles ϑ_{LF} referred to the grid angle around the fault in $t = 0,1 \text{ s} \dots 0,2 \text{ s}$.

When these are coherent, transient stability was achieved. Due to the rotor slip of induction machines this procedure is not applicable in distribution grids.

The operation point depending gradient of their rotor angle prevents this method.

A good alternative is to analyse the angles of the induced voltages \underline{u}_{qL} , because they are a uniform interface for all machine models. Due to their strong dependence on the rotor angle, transient instability can also be detected by incoherent angle developing.

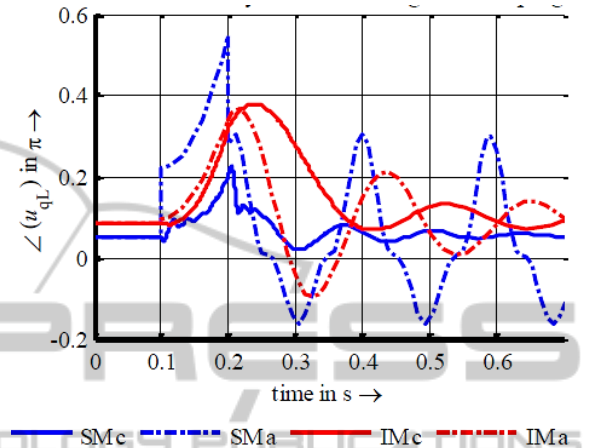


Figure 3: Angles of the voltage \underline{u}_{qL} referred to the grid angle around the fault in $t = 0,1 \text{ s} \dots 0,2 \text{ s}$.

The deviance between the models during the fault can be quite big for synchronous machines. Also the oscillation after the fault has a weak damping for the approximated models. As result only machines based on the same model can be compared quantitative. In the following sections this will be done by comparing the maximal reached angles referred to the angle of the overlying grid.

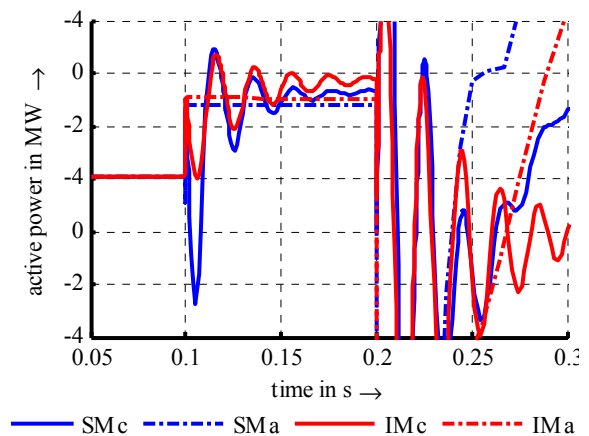


Figure 4: Absorbed active power around the fault in $t = 0,1 \text{ s} \dots 0,2 \text{ s}$ (zoom).

The deviance between the models is caused by the approximations for stator currents and rotor flux linkages. In the first part of the oscillation the

consideration of the stator currents leads to a back swing effect, which is caused by a significant consumption of active power. The active power consumption can reach significant levels due to the displacement of the short circuit currents and the resistances between the generation unit and the short circuit point. This effect is very strong for the synchronous machine. In the second part of the oscillation the approximations for the rotor flux linkages neglects the decay of active power. Please note that the active power does not jump to zero due to the resistive part of the grid impedance, which is neglectable in high voltage grids.

3.1.2 Different Durations

The duration of a short circuit in the 110-kV-grid can reach some 100 milliseconds. The time is determined by the reaction time of the protection system and potential delays for selectivity reasons.

Both machines withstand short circuit durations shorter than 200 milliseconds. Only the approximated model of the synchronous machine shows a wrong stability border.

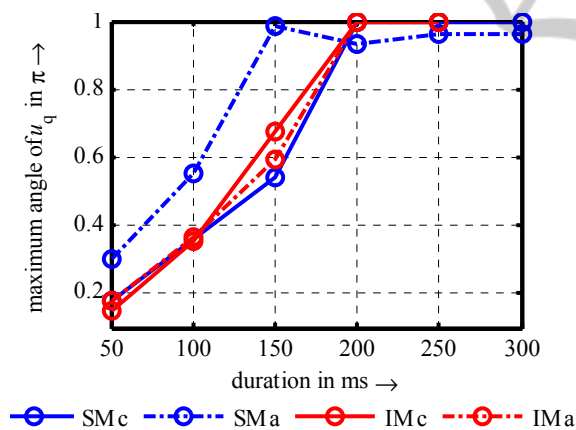


Figure 5: Maximal angles of the voltage u_{qL} in relation to the grid angle with different short circuit durations.

3.1.3 Different Residual Voltages

Depending on the real fault distance to the transformer, the voltage drop can be smaller than 100 %. Small voltage drops can also be caused by fast changes in the load flow.

All models show transient stability. In which the approximated model of the synchronous machine provided bigger values for the maximal voltage angle amplitude, whereas the approximated induction machine model provided lower values than the corresponding complete models. In the

considered scenario the approximated model for the synchronous machine works only properly with residual voltages.

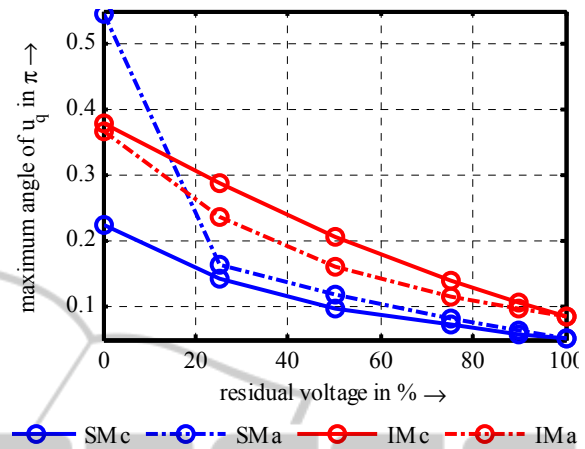


Figure 6: Maximal angles of the voltage u_{qL} in relation to the grid angle with different residual voltages.

3.1.4 Different Line Lengths

The short circuit power at the point of common coupling strongly depends on the line impedance between the transformer T1 and the generation unit.

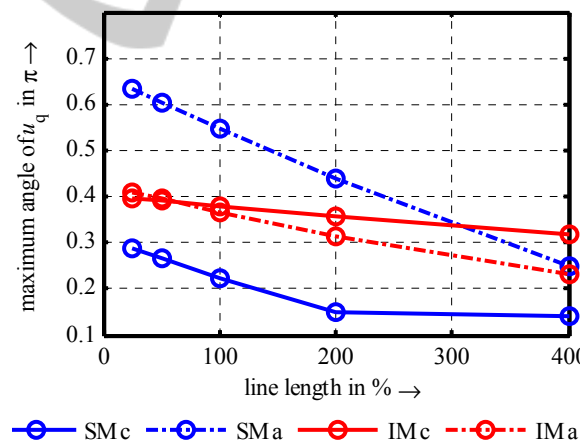


Figure 7: Maximal angles of the voltage u_{qL} in relation to the grid angle with different line lengths.

With growing line length the generation units gain transient stability. This is due to the resistive part of the line impedance, which consumes a significant amount of active power during the fault.

3.1.5 Different Rated Machine Powers

The rated power has an impact on the machine parameters. This dependence is shown here for a

range of possible values, without displaying the array of implemented parameters.

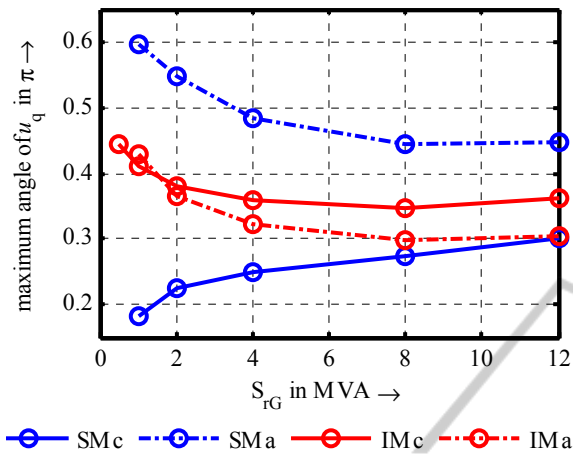


Figure 8: Maximal angles of the voltage u_{qL} in relation to the grid angle with different rated power of the machine.

With smaller rated power, the difference between the complete and the approximated synchronous machine model increase. With smaller values the transient stability for synchronous machines is enhanced and for induction machines reduced.

3.1.6 Different Operation Points

In the previous scenarios the machines were always initialized with rated power. In the classic approach this is the worst case. The transient stability is improved with lower machine utilization, because the accelerating torque is higher.

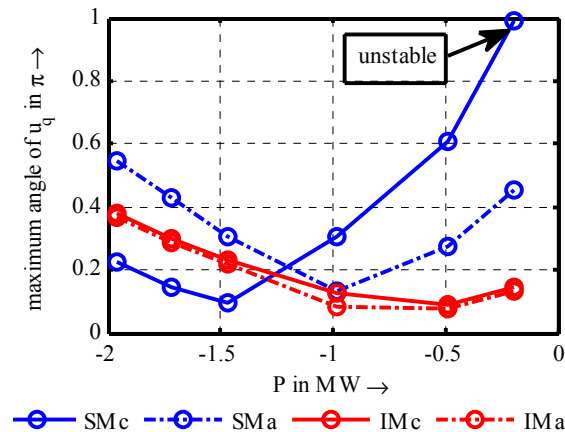


Figure 9: Maximal angles of the voltage u_{qL} in relation to the grid angle with different machine utilisation powers P .

In contrast to the high voltage grid the machine in the distribution grid can be subject to a distinct

back swing effect. This leads to an optimal operation point, which is effected by the impedance between generation unit and fault. The approximated induction machine model works very well with different operation points. The approximated synchronous machine model can pretend better results than the exact model. So the instability of the synchronous machine at 10 % could not be detected.

3.2 Low Voltage Scenario

Generation units in low voltage grids are easily affected by a short circuit. To gain transient stability in the basic scenario a residual voltage of 50 % was assumed at the fault node. This can only be done, keeping in mind the deviation of the approximated model in the medium voltage scenario with residual voltages.

3.2.1 Basic Scenario

The operation point depending gradient of the rotor angles prevents the analyses of the transient stability by the rotor angles development.

As alternative again the angles of the induced voltages u_{qL} were checked for coherence. Also the quantitative comparison will be done, by comparing the maximal reached angles referred to the angle of the overlaying grid.

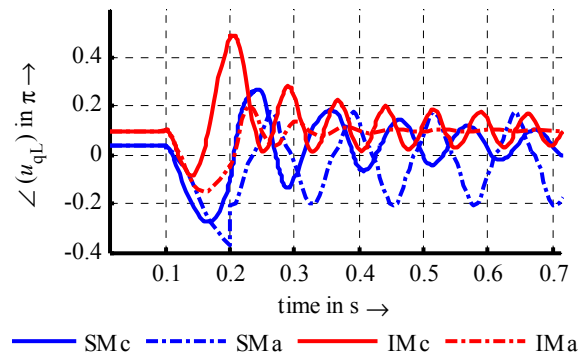


Figure 10: Angles of the voltage u_{qL} referred to the grid angle around the fault in $t = 0,1 \text{ s} \dots 0,2 \text{ s}$.

The deviance between to models is caused by the approximations for stator currents and rotor flux linkages. All models show a back swing effect, which is stronger for the approximated models. This is due to the inaccurate modelling of the active power exchange.

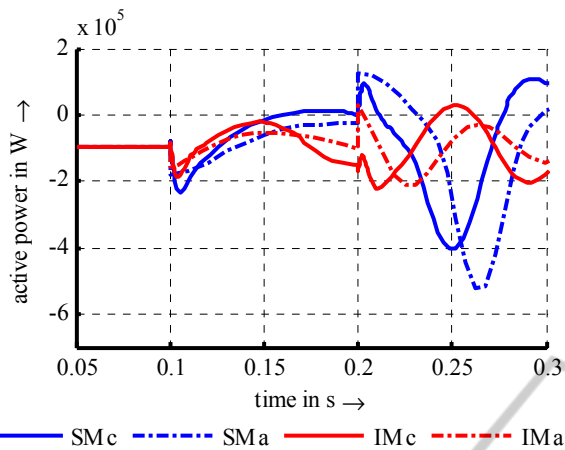


Figure 11: Absorbed active power around the fault in $t = 0,1 \text{ s} \dots 0,2 \text{ s}$ (zoom).

3.2.2 Different Durations

The short circuit duration in distribution grids can reach higher values than in the transmission grids. This is due to simpler and slower protection systems.

The induction machine withstands a short circuit durations smaller than 250 milliseconds. The approximated model is not suitable for long short circuit durations. The synchronous machine is able to reach a new stable operation point. This is due to the assumed residual voltage of 50 %.

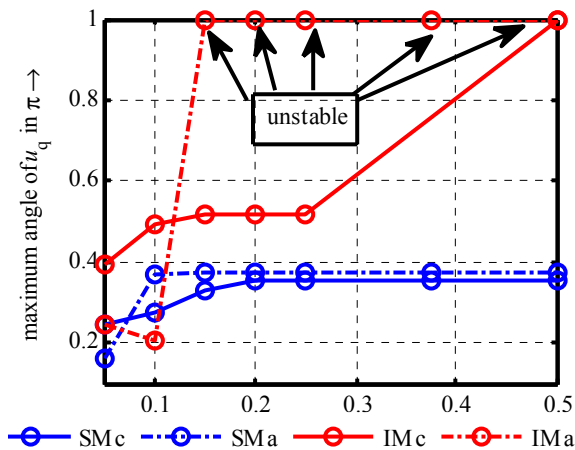


Figure 12: Maximal angles of the voltage u_{qL} in relation to the grid angle with different short circuit durations in s.

3.2.3 Different Residual Voltages

Depending on the real fault distance to the transformer, the voltage drop can be smaller than 100 %. Small voltage drops can also be caused by fast changes in the load flow.

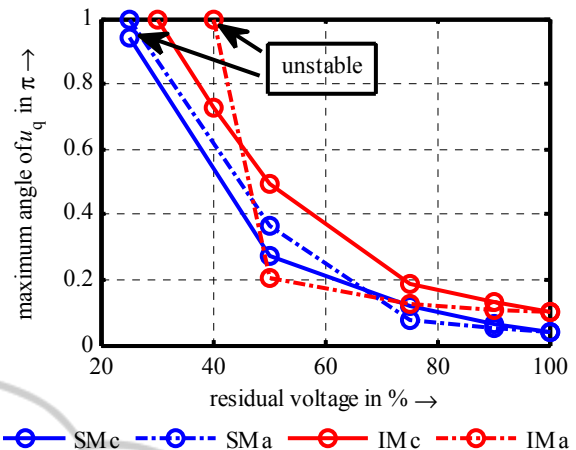


Figure 13: Maximal angles of the voltage u_{qL} in relation to the grid angle with different residual voltages.

In this scenario the models only show transient stability for significant residual voltages at the 110-kV node. The approximated models are faster to show transient instability.

3.2.4 Different Line Lengths

The short circuit power at the point of common coupling strongly depends on the line impedance between the transformer T1 and the generation unit.

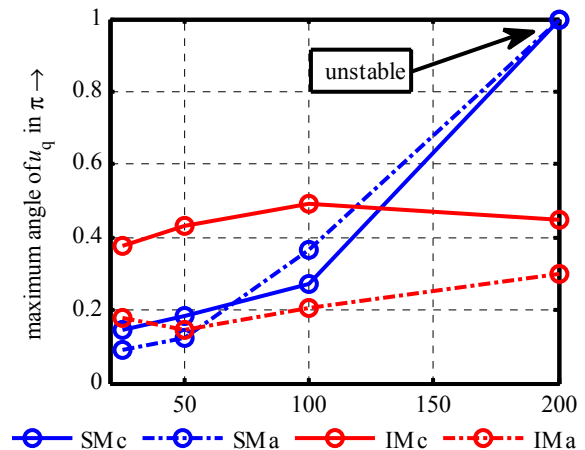


Figure 14: Maximal angles of the voltage u_{qL} in relation to the grid angle with different line lengths in %.

With bigger line length the synchronous generator loses transient stability. The approximated models are able to reproduce the effects of different short circuit impedances.

3.2.5 Different Rated Machine Powers

The rated power has an impact on the machine parameters. This dependence is shown here for a range of possible values, without displaying the array of implemented parameters.

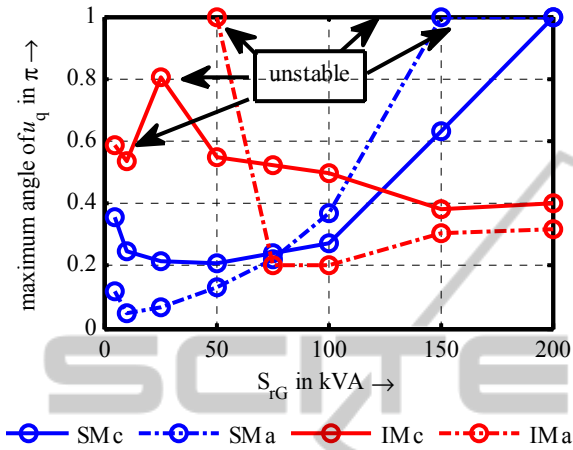


Figure 15: Maximal angles of the voltage u_{qL} in relation to the grid angle with different rated power of the machine.

With smaller rated power the difference between the complete and the approximated synchronous machine model increase. Similar to the medium voltage scenario the transient stability of synchronous machines is enhanced and for induction machines reduced with smaller values for the rated machine power.

3.2.6 Different Operation Points

In the other scenarios the machines were always initialized with rated power. In contrast to the classic model this is not the worst case.

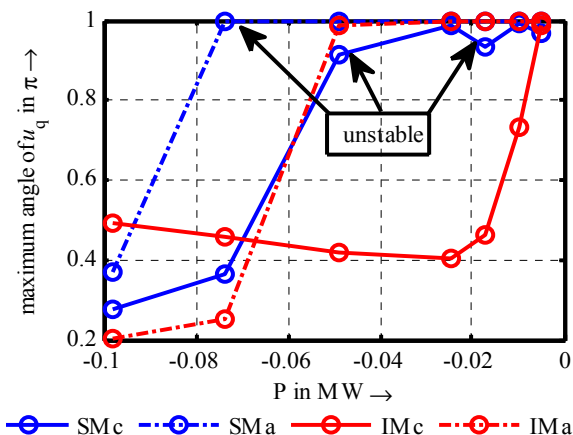


Figure 16: Maximal angles of the voltage u_{qL} in relation to the grid angle with different machine utilisation powers P .

The transient stability of synchronous and induction machine is reduced with low active power infeed, whereas the induction machine is affected at relatively low values. The approximated models show the transient instability afore.

4 CONCLUSIONS

The complete models of synchronous and induction machines were compared with selected approximated models of lower order. This is to validate the approximations for the utilisation in transient stability analysis in distribution grids.

A range of scenarios was analysed, to detect the influence of different parameters in the model accuracy. This was done comparing the maximal angle amplitude of the modelled machine voltage sources. Doing so, the temporally developing still has to be taken in to account to detect all cases of instability.

The results show that the approximated models can be used to simulate stable oscillations, but they lose their accuracy approaching the area of transient instability. They can still be used to analyse positive or negative effects on the transient stability.

The differences between the models are mostly due to the modelling of the active power exchange during fault, which is not jumping to zero as it does in high voltage scenarios.

It has to be noted that the accuracy of the models and also the transient stability strongly depend on the rated and the actual power of the generation units.

REFERENCES

- Kundur, P., 2007. *Power System Stability and Control*, Tata McGraw-Hill. New York.
- Oswald, B., 2009. *Berechnung von Drehstromnetzen*, Vieweg+Teubner. Wiesbaden.
- Hofmann, L., 2003. *Effiziente Berechnung von Ausgleichsvorgängen in ausgedehnten Elektroenergiesystemen*, Shaker Verlag. Aachen.